Hybrid Films based on Sodium Alginate and Porous Clay Heterostructures

SORINA ALEXANDRA GAREA*, ANDA IONELIA MIHAI , ADI GHEBAUR
University Politehnica of Bucharest, Faculty of Applied Chemistry and Material Science, 1-7 Gh. Polizu Str., 011061, Bucharest, Romania

The aim of this study was to point out the effect of porous clay heterostructure (PCH) and polymer concentration on thermal and dynamic mechanical properties of Sodium Alginate (SA) based hybrid films. New hybrid films based on SA and PCH were prepared by solvent casting method using different polymer concentrations and clay loadings. The interactions between nanofiller (PCH) and polymer matrix (SA), thermal stability and dynamic mechanical properties of neat SA and hybrid films were evaluated by Fourier transform infrared (FTIR) spectroscopy, thermogravimetric analysis (TGA) and dynamic mechanical analysis (DMA). The obtained results showed the influence of PCH within SA on the storage modulus and a moderate change of thermal stability, the glass transition temperature being also recorded. The concentration of SA solution and PCH are significant factors which affect the thermal and mechanical properties of hybrid films.

Keywords: sodium alginate, porous clay heterostructures, hybrid films, thermal stability, dynamic mechanical analysis

Sodium alginate (SA) is a salt of alginic acid, an anionic polysaccharide with linear structure obtained from natural source. Regarding on chemical structure SA is a copolymer based on (1-4) linked β-D-Mannuronate (M) and α-L-Guluronate (G) units [1-3]. The properties (swelling capacity, gel production, thickening effect) of SA are strongly influenced by the M and G content blocks [4].

This polymer type can be included in non-toxic, biodegradable and biocompatible polymer class, with a high swelling capacity and various applications like biomedical applications (tissue engineering, pharmaceutical field: guest for drug/proteins encapsulation, binder for medical tablets, extracellular matrix for biological studies), food industry (food thickening agent, packaging film) and agriculture [5-11].

From processability point of view SA can be processed in different ways yielding films, capsules and porous scaffolds with various applications [12, 13].

In comparison with classical polymers, neat SA exhibits some disadvantages with major impact on limiting the final applications. Low thermal stability, poor mechanical properties, strong hydrophilic character and loss of structural integrity are the main disadvantages of this polymer type [14, 15].

Some original strategies developed in order to overcome SA drawbacks were summarized in figure 1.

A method often used for designing attractive SA based systems involves combination of this polymer type with other polymers like chitosan, karragenan, polyvinyl alcohol and gelatin.

The dispersion of some micro- and nanostructured agents like layered silicates (montmorillonite (MMT), halloysite (HNT) and layered double hydroxide (LDH)), carbon nanotubes (CNT), graphene oxide (GO) and hydroxyapatite within SA was found to be another suitable method for obtaining hybrid materials with enhanced properties and special targeted applications (drug delivery field, smart hybrid scaffold, wastewater purification [16-22]. This type of hybrid materials combines the properties of polymer matrix with those of micro- or nanostructured agents [23].

Hybrid materials based on alginate and graphene oxide or CNT are used to remove different types of ionic dyes or metals from wastewaters [22]. Important progresses had been made in drug delivery field by dispersing clay minerals in alginate matrix. In some cases the clay addition within polymer matrix drastically modified the drug release profile [24, 25].

The synthesis of high performance hybrid materials based on sodium alginate and various micro- and nanostructured agents is influenced by some factors such as micro- or nanostructured agent type, compatibility of the two components, dispersion stability, surface chemistry of micro- or nanostructured agent, interactions which occurred between polymer and micro/nanostructured agent. For instance the interaction between clay mineral and alginate takes place by intermolecular hydrogen bonds and by electrostatic interactions [26].

Porous clay heterostructures are new synthetic inorganic nanostructured materials characterized by high thermal stability, high surface area and porosity. This type of material is used in wide applications like heterogeneous catalysts, molecular sieve and decontamination agent [27, 28].

The development of hybrid materials based on polymer matrix and porous clay heterostructures can be considered

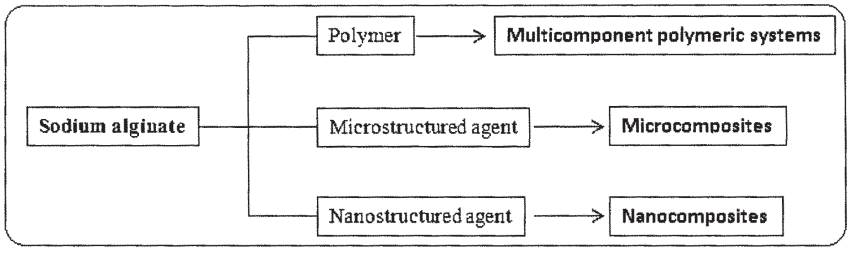

Fig.1. Strategies for improving the SA properties

* email: garea_alexandra@yahoo.co.uk; Tel.: +40214023844

a new and challenging research direction. In the literature only a few articles focused on the synthesis of hybrid materials based on polypropylene and porous clay heterostructures were reported [29].

The present study described the synthesis of new hybrid films based on Sodium Alginate and Porous Clay Heterostructures (PCH). The influence of PCH introduction within Sodium Alginate was highlighted by FTIR Spectroscopy, Thermogravimetrical analysis (TGA) and Dynamic mechanical analysis (DMA).

Experimental part

Materials and methods

A natural montmorillonite (Nanofil 116 (MMT-Na)) with a cationic exchange capacity (CEC) of 116 mEq/100 g clay was supplied from Southern Clay Products.

Alginic acid sodium salt (**SA**) from brown algae with medium viscosity, Hexadecyltrimethylammonium bromide (**HDTMA**), tetraethyl orthosilicate (**TEOS**) and dodecylamine (**DDA**) were supplied from Sigma-Aldrich and used as received.

The chemical structures of the raw materials are shown in figure 2.

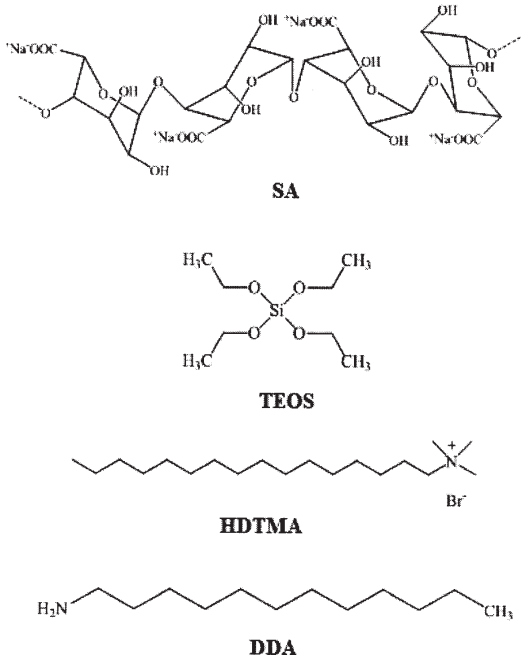

Fig.2. Chemical structures of raw materials

Synthesis of porous clay heterostructure (PCH)

The porous clay heterostructure (PCH) was synthesized using a method described in our previous paper [30]. PCH synthesis was performed in two steps which include MMT-Na organophilization with HDTMA by a cationic exchange reaction and mesoporous silica generation between modified silicate layers. PCH synthesis was done using of 1:20:120 molar ratio between MMT-HDTMA:DDA:TEOS.

5 g of modified montmorillonite with HDTMA (MMT-HDTMA) hydrated with 5 mL of demineralized water and DDA co-surfactant were stirred for 10 min at room temperature. In the next step TEOS was slowly added and the reaction mixture was maintained at room temperature under stirring for 5 h and additional 19 h without stirring. The obtained product was centrifuged, washed with ethanol, air-dried and finally subject to thermal treatment at 650°C, with a heating rate of 1°C/min to remove the organic fractions.

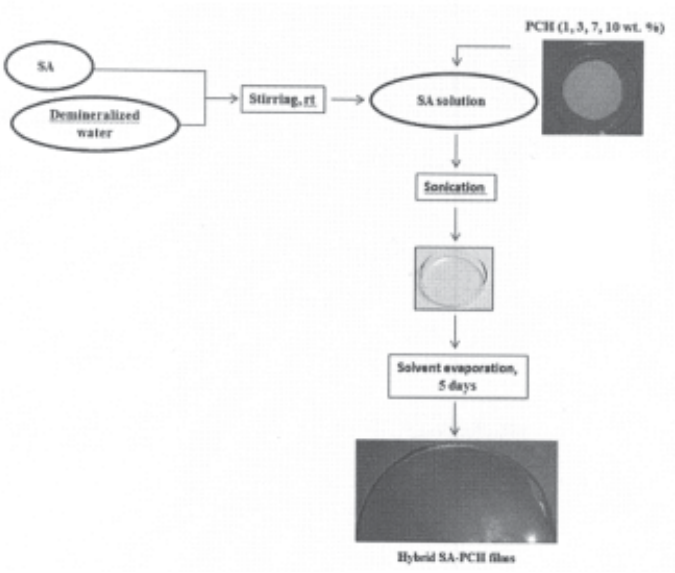

Fig. 3. Synthesis steps of hybrid films

Synthesis of hybrid films

The synthesis of hybrid films was done using the strategy schematically described in figure 3.

In the first step different SA solutions (1, 2 and 3 wt. %) were prepared by dissolving polymer in demineralized water, at room temperature under mechanical stirring. The dissolution time was dependent on SA concentration.

In the second step different PCH concentrations (1, 3, 7 and 10 wt. %) were dispersed within SA solutions by sonication for 15 minutes.

In the final step each suspension was poured into polystyrene Petri dishes and left at room temperature for 5 days for solvent evaporation.

Characterization techniques

FTIR spectra were recorded on a Bruker VERTEX 70 spectrometer using 32 scans with a 4 cm^{-1} resolution. The samples were analyzed from KBr pellets.

Dynamic mechanical analysis (DMA) tests were run on a TRITEC 2000 B using 2°C/min heating rate at 1 Hz frequency in the -60-120°C temperature range.

Thermogravimetric analysis (TGA) was performed on a Q 500 TA Instrument. The samples were heated from 20 to 920 ^{0}C at a scanning rate of 10 ^{0}C/min under a constant nitrogen flow rate.

Results and discussions

FTIR characterization

FTIR spectra were recorded in order to point out the presence of PCH within SA films and to highlight possible interactions which occurred between clay (PCH) and polymer matrix (SA).

In the first step FTIR spectra of the components involved in hybrid materials were registered. Figure 4 shows FTIR spectra of PCH and SA films synthesized by using different SA solution concentrations (1 wt. %, 2 wt. %, 3 wt. %).

The characteristic bands of PCH at 3738 cm^{-1} (OH stretching vibrations ($\nu_{Si\text{-}OH}$)), 3441 cm^{-1} (OH stretching vibrations of water molecules adsorbed on PCH) and 1086 cm^{-1} (vibrations of three dimensional silica network [**30, 31**]) are observed.

For all SA films the following FTIR peaks were identified and assigned: 3322/3325/3331cm^{-1} (OH-stretching vibrations), 2932 and 2855 cm^{-1} (C-H symmetric and asymmetric vibrations), 1600 and 1413 cm^{-1} (COO^- symmetric and asymmetric stretching vibrations). The peaks at 1086 and 1036 cm^{-1} were assigned to C-O-C

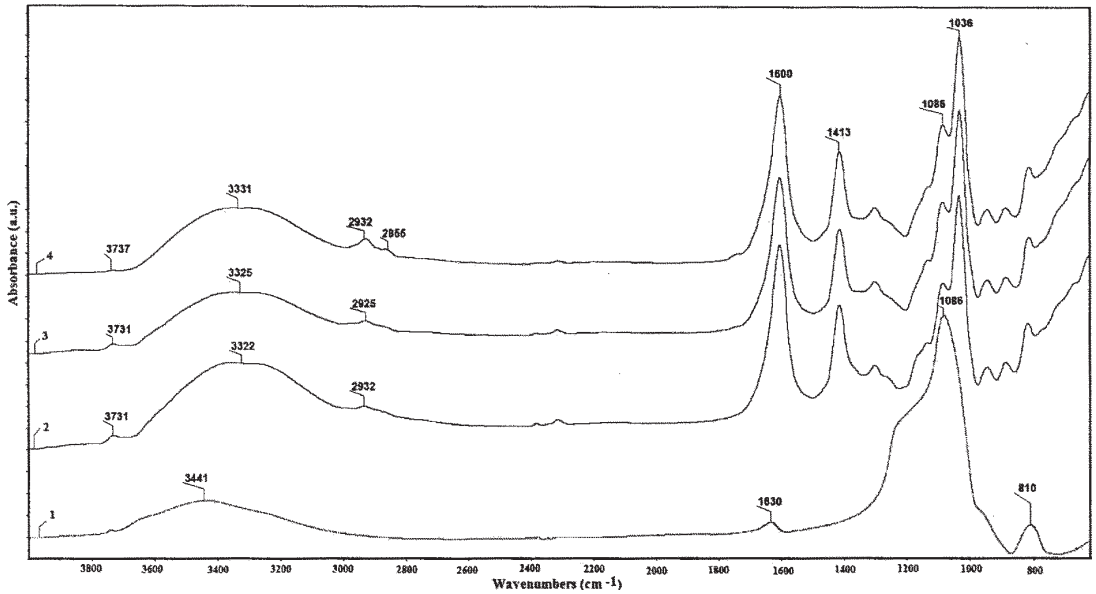

Fig. 4. FTIR spectra of 1-PCH and SA films synthesized by using different concentrations of SA solution: 2-1 wt. %, 3-2 wt. %, 4-3 wt. %

stretching vibration. Similar FTIR spectra of SA were reported in the literature [32].

The FTIR spectra of hybrid films are shown in figures 5, 6 and 7.

As one may observe from figure 5 the presence of PCH in SA films was proved by the increase of the intensity of the peak at about 1088 cm^{-1} which was found to be dependent on PCH concentration. Thus the highest peak increase was registered for SA film with a PCH 10 wt. % content. The same change was highlighted for the other hybrid films based on SA 2 wt. % and 3 wt. %.

In addition the peak assigned to OH stretching vibration was shifted to higher values for all hybrid films in comparison with neat SA films. The formation of some

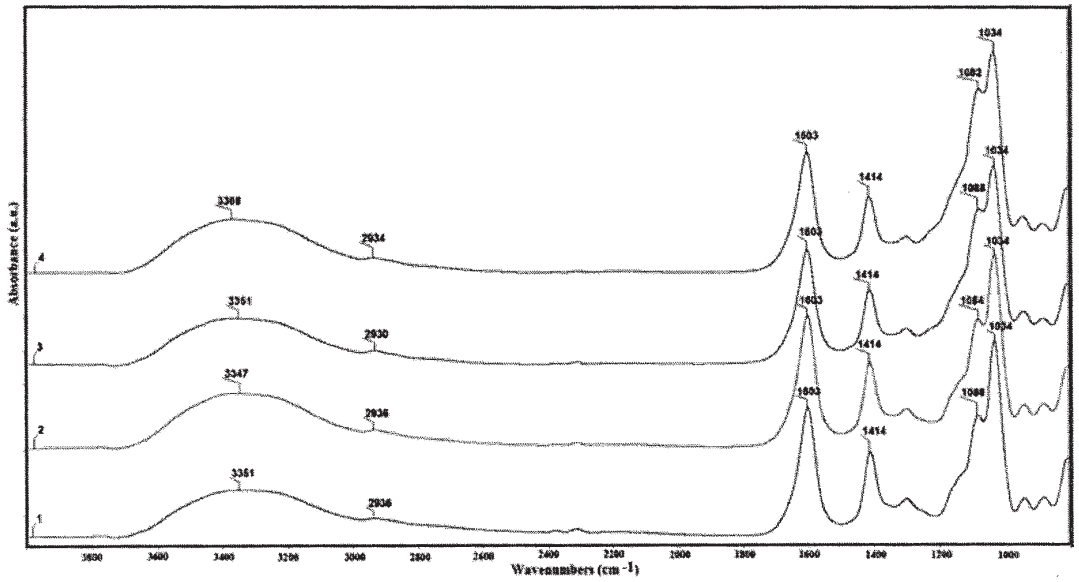

Fig. 5. FTIR spectra of hybrid films based on SA 1 wt. % and: 1-PCH-1 wt. %, 2-PCH-wt. 3%, 3-PCH-7 wt. %, 4-PCH-10. %

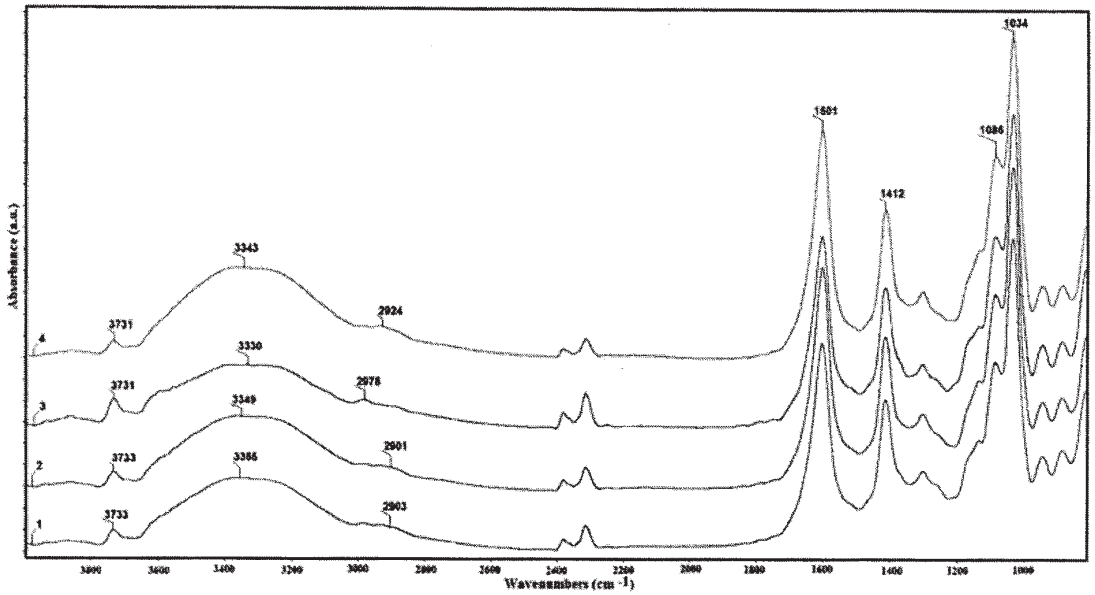

Fig. 6. FTIR spectra of hybrid films based on SA 2 wt. % and: 1- PCH-1 wt. % 2-PCH-3 wt. %, 3-PCH-7 wt. %, 4-PCH-10 wt. %

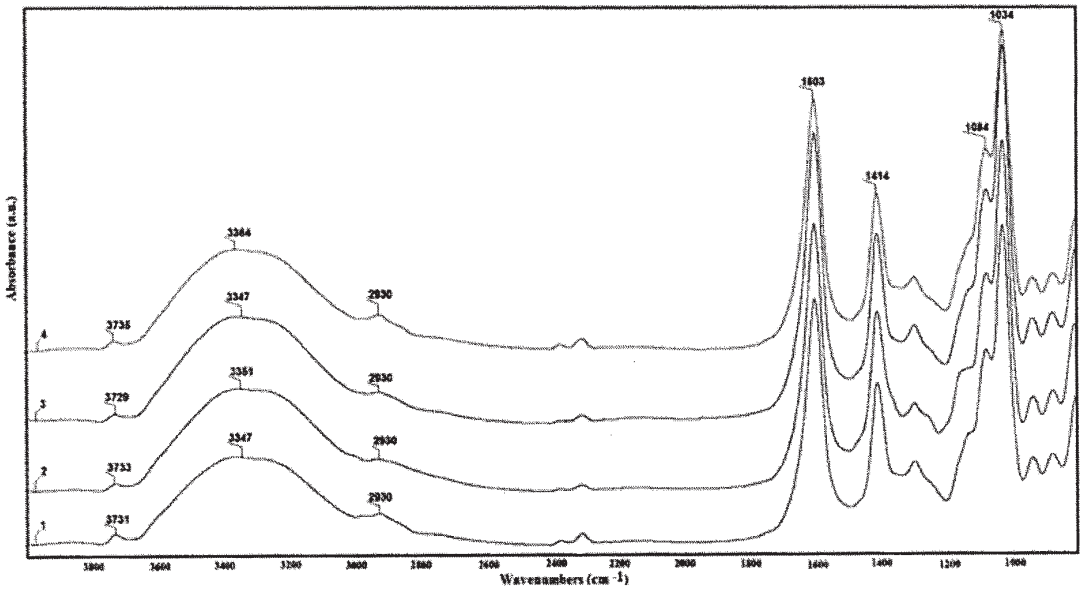

Fig. 7. FTIR spectra of hybrid films based on SA 3 wt. % and: 1- PCH-1 wt. % 2-PCH-3 wt. %, 3-PCH-7 wt. %, 4-PCH-10 wt. %

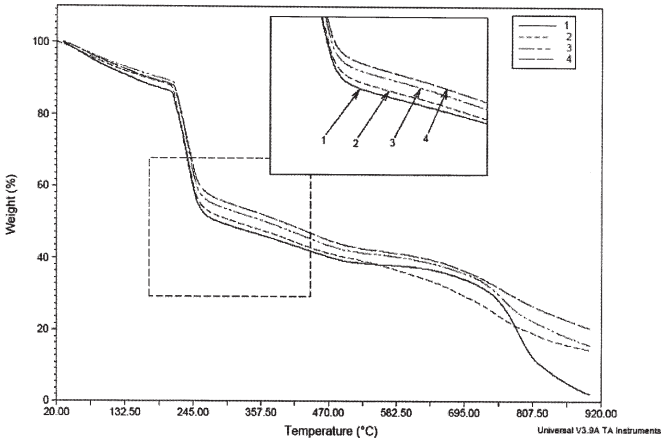

Fig. 8. TGA curves of 1- SA 1 wt. %, 2- SA 1 wt. %- PCH 1 wt. %, 3- SA 1 wt. %- PCH 7 wt. %, 4- SA 1 wt. %- PCH 10 wt. %

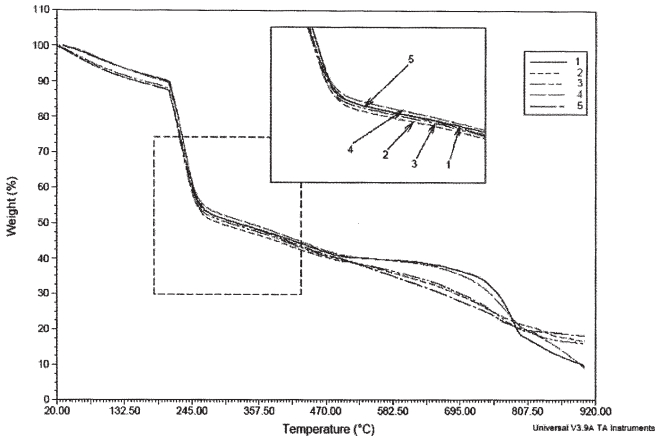

Fig. 9. TGA curves of 1- SA 2 wt. %, 2- SA 2 wt. %- PCH 1 wt. %, 3- SA 2 wt. %- PCH 7 wt. %, 4- SA 2 wt. %- PCH 10 wt. %

hydrogen bonding between SA and PCH could explain this peak shift.

Thermogravimetrical analysis

Thermal stability of the neat SA and hybrid films was studied by thermogravimetric analysis (TGA).

In figures 8, 9 and 10 the thermal degradation profiles of SA and hybrid films are shown. The TGA results were summarized in Table 1.

All neat SA films and hybrid materials have shown an initial weight loss assigned to the loss of absorbed water and a second stage corresponding to SA/hybrid decomposition which started at about 205°C.

In comparison with neat SA 1 wt. % film the hybrid materials which contain 1 wt. % PCH showed a slight increase of thermal stability. Thus $T_{onset\ 15\ \%}$ increased with 2-6°C and $T_{onset\ 40\ \%}$ with 2-12°C.

This improvement of thermal stability was assigned to barrier effect introduced by PCH presence. The polymer interpolated between PCH layers exhibits an improved thermal stability compared with neat polymer.

A similar thermal behaviour was reported for SA interpolated between organophilized montmorillonite layers [**33**].

This variation of thermal stability was found to be dependent on SA concentrations and also PCH loadings.

In case of hybrid films based on higher SA concentration (2, 3 wt. %), a low decrease of $T_{onset\ 15\ \%}$ was recorded.

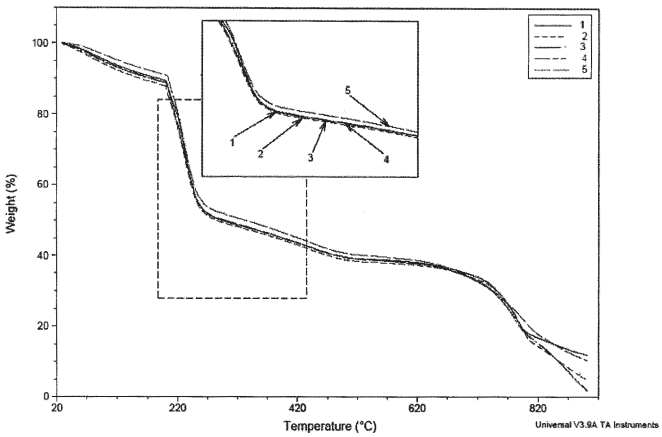

Fig.10. TGA curves of 1-SA 3 wt. %, 2- SA 3 wt. %- PCH 1 wt. %, 3- SA 3 wt. %- PCH 7 wt. %, 4- SA 3 wt. %- PCH 10 wt. %

A similar variation of thermal stability was highlighted by other authors for different hybrid materials based on SA and various nanostructured agents (graphene oxide (GO), Na-montmorillonite, organophilized montmorillonite) [6, 7, 32, 33].

Dynamic mechanical analysis (DMA)

This method was useful to study the influence of hybrid composition in terms of glass transition temperature (T_g) and storage modulus (E').

T_g values of neat SA and hybrid films were determined from Tan δ against temperature curves. Figure 11 shows

Table 1
THERMAL PROPERTIES OF NEAT SA FILMS AND SA-PCH HYBRID FILMS

Sample	$T_{onset\ 15\ \%}$ (°C)[a]	$T_{onset\ 40\ \%}$ (°C)[b]
SA 1 wt. %	*212*	*244*
SA 1 wt. %-PCH 1 wt. %	*214*	*246*
SA 1 wt. %-PCH 3 wt. %	*216*	*237*
SA 1 wt. %-PCH 7 wt. %	*218*	*251*
SA 1 wt. %-PCH 10 wt. %	*218*	*256*
SA 2 wt.%	*213*	*244*
SA 2 wt. %-PCH 1 wt. %	*211*	*244*
SA 2 wt. %-PCH 3 wt. %	*211*	*243*
SA 2 wt. %-PCH 7 wt. %	*213*	*249*
SA 2 wt. %-PCH 10 wt. %	*210*	*246*
SA 3 wt. %	*212*	*244*
SA 3 wt. %-PCH 1 wt. %	*205*	*243*
SA 3 wt. %-PCH 3 wt. %	*208*	*245*
SA 3 wt. %-PCH 7 wt. %	*205*	*241*
SA 3 wt. %-PCH 10 wt. %	*214*	*247*

[a]*temperature at 15 % weight loss*

[b]*temperature at 40 % weight loss*

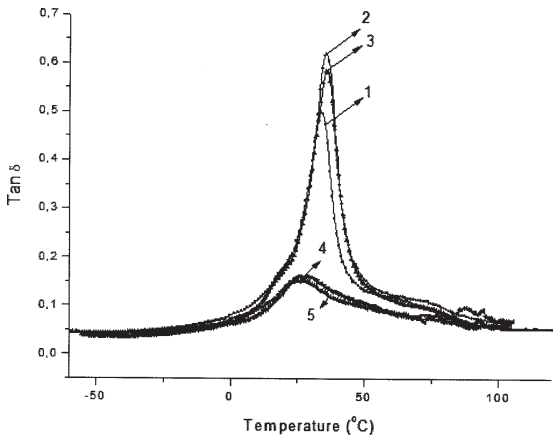

Fig.11. The dependence of Tan δ against temperature for: 1- SA 3 wt. % and hybrid films based on SA 3 wt. % and various PCH concentrations: 2-PCH 1 wt. %, 3-PCH 3 wt.%, 4-PCH 7 wt. %, 5-PCH 10 wt. %

an example of Tan δ-temperature dependence curve for hybrid materials based on SA 3 % and different PCH concentrations (1, 3, 7 and 10 wt. %).

DMA results highlighted a small decrease of T_g with 5-6 °C for hybrid films which contain higher PCH loadings (7 wt. % and 10 wt. %) and a slight increase (2 °C) of T_g for hybrid materials with a relatively low PCH content (1 wt. %, 3 wt. %).

The polymer solution viscosity could be a factor which influences the PCH dispersion within SA. Therefore T_g values were also determined for hybrid materials based on SA 1 wt.% and 2 %.

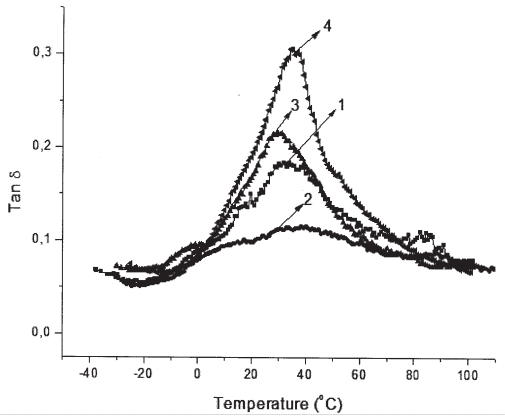

Fig.12. The dependence of Tan δ against temperature for: 1- SA 2 wt. % and hybrid films based on SA 2 wt. % and various PCH concentrations: 2-PCH 1 wt. %, 3-PCH 3 wt.%, 4-PCH 10 wt. %

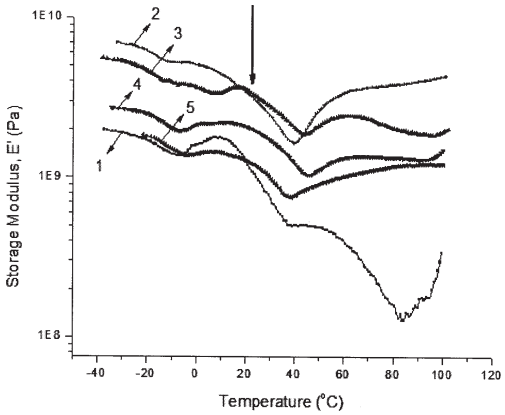

Fig.13. The dependence of Storage Modulus against temperature for 1- SA 1 wt. % and hybrid films based on SA 1 wt. % and various PCH concentrations: 2-PCH 1 wt. %, 3-PCH 3 wt.%, 4-PCH 7 wt. %, 5-PCH 10 wt. %

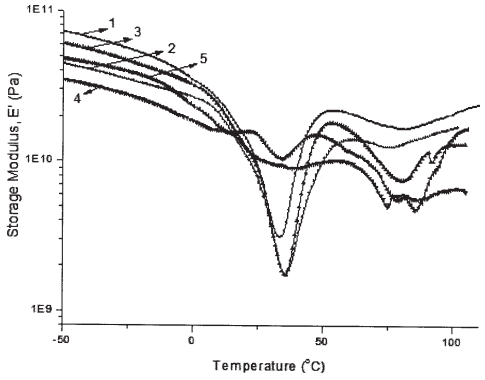

Fig.14. The dependence of Storage Modulus against temperature for 1- SA 3 wt. % and hybrid films based on SA 3 wt. % and various PCH concentrations: 2-PCH 1 wt. %, 3-PCH 3 wt.%, 4-PCH 7 wt. %, 5-PCH 10 wt. %

As one may notice from figure 12 the hybrid materials based on SA 2 wt. % exhibit a slight increase of T_g value with about 3-5 °C even at high PCH concentrations in comparison with neat SA film.

Similar results were obtained for hybrid materials based on SA with the lowest concentration (1 wt. %).

The influence of PCH on storage modulus of SA films was highlighted from Storage Modulus against temperature curves (figs. 13-15).

The presence of PCH within SA 1 wt. % based films favoured an increase of storage modulus even for high PCH concentration (7 wt. %) which may be attributed to PCH acting in this case as a reinforcing agent. The low concentration of SA solution allowed a good dispersion of PCH and therefore the agglomeration tendency was

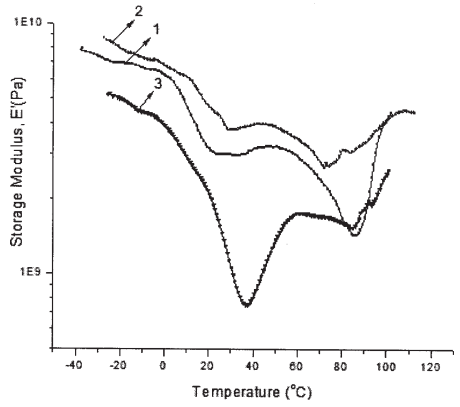

Fig.15. The dependence of Modulus against temperature for 1- SA 2 wt. % and hybrid films based on SA 2 wt. % and various PCH concentrations: 2-PCH 1 wt. %, 3- PCH 10 wt. %

minimized. At higher PCH concentrations (10 wt. %) a decrease of storage modulus was recorded probably due to the PCH agglomeration which diminished its reinforcing effect.

The DMA results highlighted also a significant influence of SA solution concentration on dynamic mechanical properties (especially for storage modulus). The increase of SA solution concentration ensures higher viscosity which hinders PCH dispersion. In case of hybrid materials based on SA 3 wt. % the PCH loses the effect of reinforcing agent (fig. 14).

In this case a decrease of storage modulus was recorded. The high viscosity of SA solution does not favor uniform dispersion of PCH and an agglomeration tendency occurred. We concluded that in this case PCH acts as a plasticizing agent.

Also for hybrid films based on SA 2 wt. % an increase of storage modulus was recorded only for lower PCH concentrations (1 wt. %).

Conclusions

New hybrid materials based on SA and PCH were successfully prepared by solvent casting method.

SA solution concentration and PCH loading were found to be two main factors which influence the hybrid films properties (thermal stability, glass transition temperature, storage modulus).

FTIR results highlighted the presence of some interactions (hydrogen bonding formation) between SA and PCH which proved that PCH exhibits a reactive surface.

The incorporation of low concentration (1 wt.%) of PCH within SA exhibits a beneficial effect on thermal stability. This improvement of thermal stability was assigned to barrier effect introduced by PCH presence.

DMA results indicated that the PCH introduction favoured an increase of storage modulus of SA films, especially for low concentration of SA solution (1 wt. %).

The introduction of higher PCH concentrations (10 wt. %) caused a decrease of storage modulus probably due to the PCH agglomeration which diminishes its reinforcing effect.

Acknowledgements: Executive Agency for Higher Education, Research, Development and Innovation Funding (UEFISCDI) and National Research Council (CNCS) are gratefully acknowledged for the financial support for the PN II research project: DRUG DELIVERY HYBRIDS BASED ON POLYMERS AND POROUS CLAY HETEROSTRUCTURES (DELPOCLAY), No. 154/2012.

References

1.BIERHALZ, A.C.K., DA SILVA, M.A., BRAGA, M.E.M., SOUSA, H.J.C., KIECKBUSCH T.G., LWT - Food Sci. and Tech., **57**, 2014, p. 494.
2. SHEN, W., HSIEH, Y-LO., Carbohydrate Polym., **102**, 2014, p. 893.
3. MALESU KUMAR, V., SAHOO, D., NAYAK, P.L., Int. J. of Appl. Biology and Pharma. Tech., **2**, 2011, p. 402.
4. YANGA, L., MAB, X., GUOA, N., ZHANGAA, Y., Carbohydrate Polym., **105**, 2014, p. 351.
5. LIAKOSA, I., RIZZELLOA, L., BAYERA, I.S., POMPAA, P.P., CINGOLANIB, R., ATHANASSIOUA, A., Carbohydrate Polym., **92,** 2013, p. 176.
6. IONITA, M., PANDELE, M.A., IOVU, H., Carbohydrate Polym., **94**, 2013, p. 339.
7. NIE, L., LIU, C., WANG, J., SHUAI, Y., CUI, X., LIU, L., Carbohydrate Polym., **117**, 2015, p. 616.
8. XIAO, Q., GU, X., TAN, S., Food Chem., **164**, 2014, p. 179.
9. LIAKOSA, I., RIZZELLOB, L., SCURRC, D.J., POMPAB, P.P., BAYERA, I.S., ATHANASSIOUAA, A., Int. J. of Pharma., **463,** 2014, p 137.
10. KHUATHAN, N., PONGJANYAKUL, T., Int. J. of Pharma., **460**, 2014, p. 63.
11. CROSSINGHAM, Y.J., KERR, P.G., KENNEDY, R.A., Int. J. of Pharma., **473**, 2014, p. 259.
12. LI, Z., RAMAY HASSNA, R., HAUCH KIP, D., XIAO, D., ZHANG, M., Biomaterials, **26**, 2005, p. 3919.
13. CORADIN, T., NASSIF, N., LIVAGE, J., Appl. Microbiol. Biotechnol., **61**, 2003, p. 429.
14- ALBOOFETILEH, M., REZAEI, M., HOSSEINI, H., ABDOLLAHI, M., J. of Food Engineering, **117**, 2013, p. 26.
15-SHARMA, S., SANPUI, P., CHATTOPADHYAY, A., GHOSH, S.S., RSC Advances, **2,** 2012, p. 5837.
16. ELY, A., BAUDU, M., BASLY, J-P., OULD SID'AHMED, M., KANKOU, O., Journal of Hazard. Mater., **171**, 2009, p. 405.
17. LOPEZ, M.S-P., LEROUX, F., MOUSTY, C., Sensors and Actuators B: Chem., **150**, 2010, p. 36.
18. BOISSIČRE, M., ALLOUCHE, J., CHANÉAC, C., BRAYNER, R., DEVOISSELLE, J-M., LIVAGE, J., CORADIN, T., Int. J. of Pharma, **344**, 2007, p. 128.
19. SUN, L., FUGETSU, B., Chem. Engineering J., **240**, 2014, p. 565.
20. LI, Y., SUI, K., LIU, R., ZHAO, X., ZHANG, Y., LIANG, H., XIA, Y., Energy Procedia, **16**, 2012, p. 863.
21. TAMPIERI, A., SANDRI, M., LANDI, E., CELOTTI, G., ROVERI, N., MATTIOLI-BELMONTE, M., VIRGILI, L., GABBANELLI, F., BIAGINI, G., Acta Biomater., **1**, 2005, p. 343.
22. ALGOTHMI, W.M., BANDARU, N.M., YU, Y., SHAPTER, J.G., ELLIS, A.V., J. of Colloid and Interface Sci., **397**, 2013, p. 32.
23. AMER, W., ABDELOUAHDI, K., RAMANANARIVO, H.R., FIHRI, A., EL ACHABY, M., ZAHOUILY, M., BARAKAT, A., DJESSAS, K., CLARK, J., SOLHY, A., Mater. Sci. and Engineering: C, **35**, 2014, p. 341.
24. MANDAL, S., PATIL, V.S., MAYADEVI, S., Micropor. and Mesopor. Mater., **158**, 2012, p. 241.
25. PONGJANYAKUL, T., RONGTHONG, T., Carbohydrate Polym., **81**, 2010, p. 409.
26. ILIESCU, R.I., ANDRONESCU, E., GHITULICA, C.D., VOICU, G., FICAI, A., HOTETEU, M., Int. J. of Pharma., **463**, 2014, p. 184.
27. GALARNEAU, A., BARODAWALLA, A., PINNAVAIA, T.J., Nature, **374,** 1995, p. 529.
28. KOOLI, F., Micropor. and Mesopor.Mater., **184**, 2014, p.184.
29. SRITHAMMARAJ, K., MAGARAPHAN, R., MANUSPIYA, H., Packaging Tech. and Sci., **25**, 2012, p. 63.
30. GÂREA, S.A., MIHAI, A., VASILE, E., VOICU, G., Rev. Chim.(Bucharest), **65**, no. 6, 2014, p. 649.
31. PALKOVA, H., MADEJOVA, J., ZIMOWSKA, M., SERWICKA, E.M., Micropor. and Mesopor.Mater., **127**, 2010, p. 237.
32. TEZCAN, F., GUNISTER, E., OZEN, G., ERIM, F.B.,Int. J. of Biological Macromolecules, **50** , 2012, p. 1165.
33. ABOU TALEB, M.F., HEGAZY, D.E., ISMAIL, SAHAR, A., Carbohydrate Polym., **87**, 2012, p. 2263

Manuscript received: 3.12.2014